Surface outgrowths on sputtered $YBa_2Cu_3O_{7-x}$ films: A combined atomic force microscopy and transmission electron microscopy study

A. Catana,[a] J. G. Bednorz, Ch. Gerber, J. Mannhart, and D. G. Schlom[b]
IBM Research Division, Zurich Research Laboratory, 8803 Rüschlikon, Switzerland

(Received 2 December 1992; accepted for publication 10 May 1993)

We have structurally and morphologically characterized the surface of sputtered $YBa_2Cu_3O_{7-x}$ films on (001) $SrTiO_3$ using atomic force microscopy and transmission electron microscopy. Atomic force microscopy reveals three types of outgrowths with different shapes and heights between 2 and 200 nm: type I exhibits cubic habit, type II tabular habit, and type III is an agglomerate of no particular shape. Some of the type-III outgrowths are located at the center of growth spirals where the screw dislocation intersects the film surface, suggesting that in $YBa_2Cu_3O_{7-x}$ films these defects promote the occurrence of one another. Using high-resolution electron microscopy and electron diffraction the surface outgrowths have been identified as follows: type I is Y_2O_3, type II Y_2O_3 and $CuYO_2$, and type III $YBa_2Cu_3O_{7-x}$, CuO, and Y_2O_3. In contrast to types-I and -II outgrowths which are both epitaxially related to the surrounding $YBa_2Cu_3O_{7-x}$, the large type-III agglomerates consist of epitaxial and nonepitaxial grains. As it is found that the outgrowing nonepitaxial phases emanate from screw dislocations and from *a,b*-axis domain boundaries, it is suggested that both internal stresses and high interfacial energies promote such outgrowths on $YBa_2Cu_3O_{7-x}$ films.

Analysis of the surface morphology and of embedded microstructural features in $YBa_2Cu_3O_{7-x}$ (YBCO) films has provided valuable clues for the understanding of film growth mechanisms.[1-4] Surface morphology and bulk microstructure are also essential aspects for the growth and investigation of multilayers as well as for microelectronic applications.

Previous studies have shown that outgrowths formed on $YBa_2Cu_3O_{7-x}$ films and other surface features are sensitive to composition and deposition conditions,[5-7] but have not identified the structure of the out-growing second phases. Off-stoichiometry is also present inside the films, where it causes line and point defects, stacking faults, and precipitates.[4,8-12] Recently, by using scanning electron microscopy (SEM) and transmission electron microscopy (TEM), Ramesh and co-workers found that surface outgrowths ($YBa_3Cu_2O_{7-x}$) and *a,b*-axis domains are correlated in sputtered and laser-ablated YBCO films.[13] In other work it was found that films with a high density of growth spirals contain a high number of Y_2O_3 precipitates.[4] All these investigations suggest a close connection between surface features and the bulk structure of the films.

In this letter, atomic force microscopy (AFM) and TEM studies of surface outgrowths on sputtered YBCO films are presented. The shape and composition of three types of outgrowths are identified and their epitaxial orientations and the connection to the surface microstructure are discussed.

The YBCO films, about 100 nm thick, were grown by dc hollow cathode magnetron sputtering on $SrTiO_3$(001) substrates at substrate heater block temperatures (T_{sub}) of approximately 750 °C. The sputtering pressure was 650 mTorr (Ar/O_2=2:1), the plasma discharge was operated at 450 mA and 150–170 V, and after growth, the films were cooled to room temperature within an hour in 0.5 bar of O_2.

AFM images were obtained with a commercially available instrument (Nanoscope III, Digital Instruments) using optical beam deflection to monitor the displacement of a microfabricated Si_3N_4-type cantilever having a spring constant of 0.1 N/m. Images were recorded in the constant force mode with typical forces of 10^{-8} N between tip and sample.

TEM samples of the same films analyzed by AFM were prepared for both planar and cross-sectional views by standard mechanical polishing and subsequent ion milling with liquid nitrogen cooling. The observations were made on a JEOL JEM-2010 operated at 200 kV.

Figure 1 shows AFM images of the film surface which emphasize the presence of three typical surface outgrowths. Type-I outgrowths, as labeled in Fig. 1, are small precipitates densely distributed ($\simeq 10^{10}$/cm^2) over the film surface. The size of these precipitates is about (20–25) $\times$ (20–25) $\times$ (2–8) nm.[3] Type-II outgrowths [typically (200–300) $\times$ (170–230) $\times$ (30–50) nm^3] have a characteristic tabular habit and are preferentially oriented with the long edges parallel to the in-plane ⟨100⟩ axes of the film (Fig. 1), suggesting that these orientations are energetically favorable. Type-III outgrowths (Fig. 1) are large agglomerates with typical heights of 200 nm. Although the majority of the constituent grains of type-III outgrowths have irregular shapes, in most cases a platelet-like grain (A in Fig. 1) separates them from the surrounding YBCO matrix. The center of growth spirals has been observed to be a second nucleation site (B in Fig. 1), suggesting a correlation between screw dislocations and the nucleation and agglomeration of second phases.

To identify the structure of the various types of out-

[a]Present address: EPFL, Prospective and Research, 1015 Lausanne, Switzerland.
[b]Present address: Department of Materials Science and Engineering, The Pennsylvania State University, University Park, PA 16802-5505.

 0003-6951/93/63(4)/553/3/$6.00

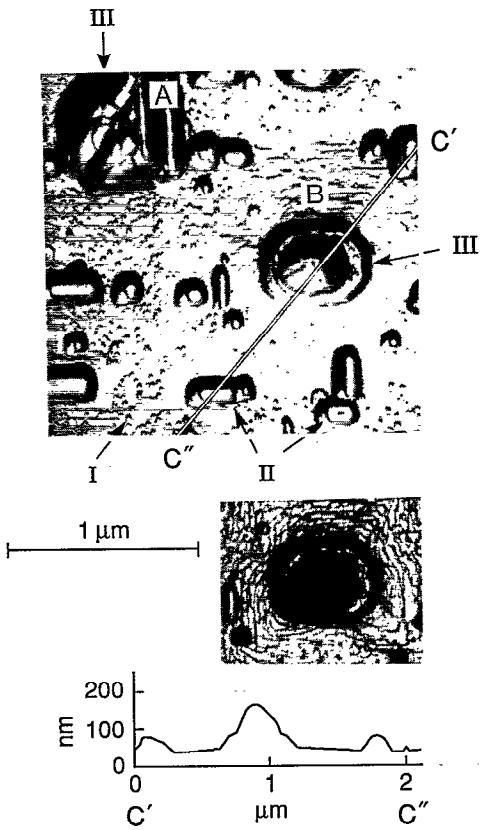

FIG. 1. AFM image of the YBCO film surface showing densely distributed outgrowths of types I–III (arrows). A refers to the YBCO platelets and B to a growth spiral. The growth spiral is shown once more in the small micrograph, in which the growth steps (one unit cell high) are clearly visible. At the bottom a height profile along the line C′–C″ is shown.

growths, high-resolution electron microscopy (HREM) and electron diffraction were employed.

Type-I particles are epitaxial Y_2O_3 grains of cube shape. Their orientation with respect to YBCO is ⟨100⟩ Y_2O_3‖ ⟨110⟩ YBCO and {001} Y_2O_3‖ (001) YBCO, in agreement with previous studies.[4,10] A cross-sectional HREM micrograph of a Y_2O_3 surface precipitate is shown in Fig. 2. Occasionally, Y_2O_3 outgrowths with {110} planes parallel to (001) YBCO nucleate in the bulk of the film. In this case they frequently separate *c*-axis from *a,b*-axis YBCO regions as shown in Fig. 3. Owing to favorable matching conditions between {110} Y_2O_3 and (001) YBCO, the presence of (001) planes of YBCO parallel to the substrate normal favors the nucleation and enhances the growth rate of Y_2O_3 with this particular orientation, as suggested previously.[14]

Y_2O_3 precipitates oriented in the latter manner ({110} Y_2O_3‖ (001) YBCO) occur on the film surface, and together with $CuYO_2$ precipitates give rise to the type-II surface features. $CuYO_2$ grows with its [421] axis parallel to [001] YBCO (Fig. 4), which is different from previously reported results.[11] Just as the nucleation of Y_2O_3 precipitates has been explained on the basis of lattice-matching arguments,[4,14] the orientation of $CuYO_2$ also relates to lattice match. Indeed, the observed orientation relationship is

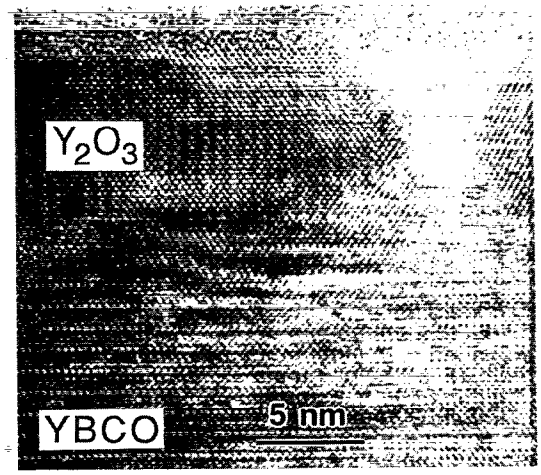

FIG. 2. Cross-sectional HREM micrograph of an epitaxial Y_2O_3 surface precipitate with the orientational relationship: {001} Y_2O_3‖ (001) YBCO, {110} Y_2O_3‖ {100} YBCO.

such that (112) and (012) $CuYO_2$ planes are almost parallel to (110) YBCO planes, the mismatch being only 1.2%. In addition to these two phases, diffraction patterns indicate the presence of other phases not yet identified.

The larger polycrystalline agglomerates (type-III outgrowths) consist of both epitaxial and nonepitaxial grains. They are predominantly correlated with YBCO *a,b*-axis plates (Fig. 5), which may serve as nucleation sites, or are located at the center of growth spirals, which were identified by AFM and scanning tunneling microscopy (Fig. 1). Different diffraction patterns obtained on the constituent grains of the agglomerates provide evidence for epitaxial grains, namely YBCO (i.e., the *a,b*-axis platelets mentioned above), CuO and Y_2O_3, as well as for unidentified constituents.

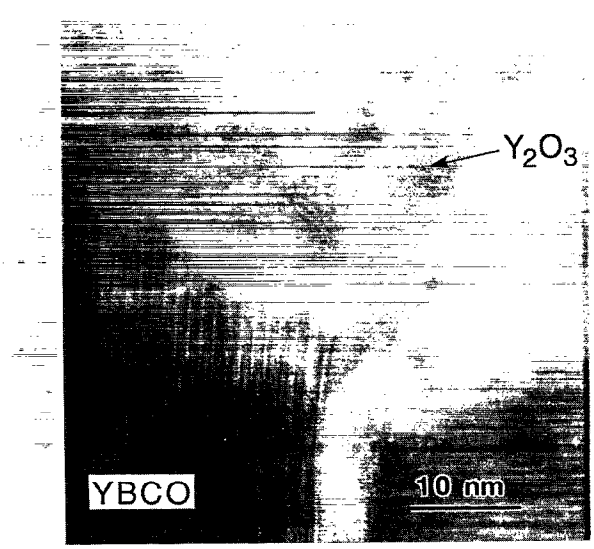

FIG. 3. Cross-sectional HREM micrograph of an epitaxial Y_2O_3 outgrowth at a domain boundary between *a,b*-axis YBCO (on the left) and *c*-axis YBCO (on the right) with {110} Y_2O_3‖ (001) YBCO and {100} Y_2O_3‖ {100} YBCO of the *a,b*-axis YBCO domain.

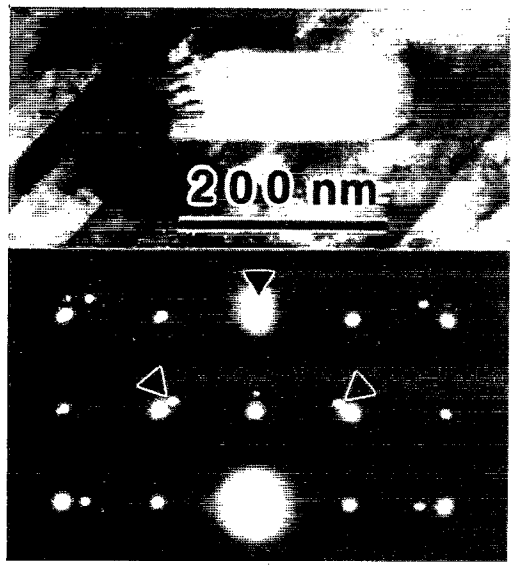

FIG. 4. Planar-view HREM micrograph of a $CuYO_2$ precipitate and corresponding selected area diffraction pattern. The epitaxial orientation is such that [001] YBCO|| [421] $CuYO_2$, (100) YBCO|| ($\bar{1}20$) $CuYO_2$. Arrows indicate 421 $CuYO_2$ reflections.

The locations and the structure of type-III precipitate agglomerates are correlated with *a,b*-axis outgrowths and with the intersections of screw dislocations with the film surface, suggesting that these defects promote one another. Precipitates have been shown to cause the nucleation of screw dislocations in the growth of other layered materials.[15,16] High interfacial energies and internal stresses between nonepitaxial precipitates and the YBCO matrix provide a driving force for the transport of impurity species to energetically more favorable nucleation or attachment sites, for example, to locations where defects such as dislocations, grain boundaries, or out-of-phase boundaries intersect the film surface. Surface outgrowths, induced by compressive stresses, are known to occur in thin films; these stresses are relieved by the transport of material along easy diffusion paths given by the defects mentioned above to unstressed regions.[17] In addition, outgrowths may form adjacent to already existing outgrowths of a different type, for example, at *a,b*-axis YBCO domains which provide favorable nucleation sites.[14]

In summary, three types of outgrowths, which are predominantly epitaxial with respect to the YBCO matrix, have been observed by AFM on sputtered YBCO films grown on (001) $SrTiO_3$. Type I are cube-shaped Y_2O_3 grains, type II have tabular habit and consist of either Y_2O_3 or $CuYO_2$ precipitates, whereas type III are agglomerate in which YBCO, CuO, and Y_2O_3 grains have been identified. Type-III outgrowths are correlated with *a,b*-axis platelets or with the center of growth spirals. These results show that *a/c*-domain boundaries and screw dislocations are favorable sites for the nucleation and agglomeration of second phases and suggest that such outgrowths on $YBa_2Cu_3O_{7-x}$ films are promoted by high interfacial energies and by internal stress.

The authors gratefully acknowledge R. F. Broom for his valuable aid, P. Chaudhari for fruitful discussions, and the Swiss National Science Foundation for financial support.

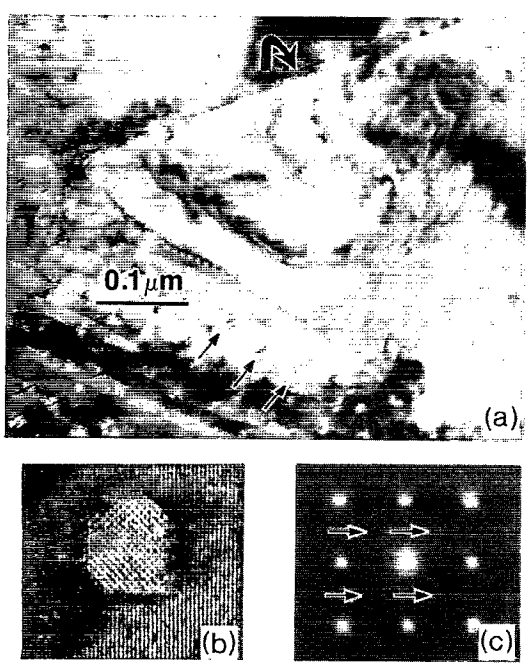

FIG. 5. (a) Planar-view TEM micrograph demonstrating the coexistence of small Y_2O_3 particles (type I) and larger agglomerates (type III). Three Y_2O_3 precipitates are marked by the parallel arrows. A YBCO platelet separating the agglomerate from the film matrix is indicated by the curved arrow. (b) HREM image of a typical Y_2O_3 precipitate and (c) corresponding selected area diffraction pattern (the four arrows indicate 100 Y_2O_3 reflections).

[1] Ch. Gerber, D. Anselmetti, J. G. Bednorz, J. Mannhart, and D. G. Schlom, Nature **350**, 279 (1991).
[2] M. Hawley, I. D. Raistrick, J. G. Beery, and R. J. Houlton, Science **251**, 1587 (1991).
[3] D. G. Schlom, D. Anselmetti, J. G. Bednorz, R. F. Broom, A. Catana, T. Frey, Ch. Gerber, H.-J. Güntherodt, H. P. Lang, and J. Mannhart, Z. Phys. B **86**, 163 (1992).
[4] A. Catana, R. F. Broom, J. G. Bednorz, J. Mannhart, and D. G. Schlom, Appl. Phys. Lett. **60**, 1016 (1992).
[5] J. A. Edwards, N. G. Chew, S. W. Goodyear, S. E. Blenkinsop, and R. G. Humphries, J. Less-Common Metals **164**, 414 (1990).
[6] J. Zhao, C. S. Chern, Y. Q. Li, P. Norris, B. Gallois, B. Kear, X. D. Wu, and R. E. Münchausen, Appl. Phys. Lett. **58**, 2839 (1991).
[7] C. C. Chang, X. D. Wu, R. Ramesh, X. X. Xi, T. S. Ravi, T. Venkatesan, D. M. Hwang, R. E. Münchausen, S. Foltyn, and N. S. Nogar, Appl. Phys. Lett. **57**, 1814 (1990).
[8] F. K. LeGoues, Philos. Mag. B **57**, 167 (1988).
[9] O. Eibl and B. Roas, J. Mater. Res. **5**, 2620 (1990).
[10] P. Lu, Y. Q. Li, J. Zhao, C. S. Chern, B. Gallois, P. Norris, P. Kear, and F. Cosandey, Appl. Phys. Lett. **60**, 1265 (1992).
[11] A. F. Marshall, V. Matijasevic, P. Rosenthal, K. Shinohara, R. H. Hammond, and M. R. Beasley, Appl. Phys. Lett. **57**, 1158 (1990).
[12] T. I. Selinder, U. Helmersson, Z. Han, J.-E. Sundgren, H. Sjöström, and L. R. Wallenberg, Physica C **202**, 69 (1992).
[13] R. Ramesh, A. Inam, D. M. Hwang, T. D. Sands, C. C. Chang, and D. L. Hart, Appl. Phys. Lett. **58**, 1557 (1991).
[14] A. Catana, D. G. Schlom, J. Mannhart, and J. G. Bednorz, Appl. Phys. Lett. **61**, 720 (1992).
[15] A. Baronnet, J. Cryst. Growth **19**, 193 (1973).
[16] M. I. Kozlovskii, Sov. Phys. Crystallogr. **3**, 206 (1958).
[17] P. Chaudhari, J. Appl. Phys. **45**, 4339 (1974).